European Radiology (2019) 29:5197–5204
https://doi.org/10.1007/s00330-019-06085-z

MAGNETIC RESONANCE

MRI for prostate cancer: can computed high *b*-value DWI replace native acquisitions?

Salma Jendoubi[1] · Mathilde Wagner[2,3] · Sarah Montagne[1,2] · Malek Ezziane[2] · Julien Mespoulet[1] · Eva Comperat[4,5] · Candice Estellat[6] · Amandine Baptiste[6] · Raphaele Renard-Penna[1,2,5]

Received: 20 October 2018 / Revised: 3 January 2019 / Accepted: 8 February 2019 / Published online: 18 March 2019

Abstract

Objective To compare computed high *b*-value diffusion-weighted images (c-DWI) derived from low *b*-value DWI images and acquired high *b*-value DWI (a-DWI), in overall image quality and prostate cancer detection rate.

Materials and methods A total of 124 consecutive men with suspected prostate cancer (PCa) underwent diagnosis prostate MRI on a 3.0 T MR system using a 32-channel phased-array torso coil. Among them, 63 underwent prostate biopsy. MRI protocol included 3DT2w images, high resolution Fov Optimized and Constrained Undistorted Single-Shot (FOCUS™) DWI images with *b*-values of 100, 400, 800, and 2000 s/mm^2 and dynamic contrast enhanced images. C-DWI images (2000 and 2500 s/mm^2) were derived from the three lower acquired *b*-value DWI images using a mono-exponential diffusion decay. C-DWI and acquired high *b*-value DWI (a-DWI) (2000 s/mm^2) were compared for image quality (background signal suppression, anatomic clarity, ghosting, distortion) and tumor conspicuity by four radiologists.

Results C-DWIs demonstrated higher rating than a-DWIs for overall image quality despite worsened ghosting. In patients with a biopsy, similar detection rate was observed while conspicuity was better with c-DWI ($p < 0.001$). Non-acquisition of high *b*-value a-DWI reduced total acquisition time by 220 s per patient.

Conclusion C-DWI provides a substantial reduction in acquisition time while maintaining comparable prostate cancer detection rate and improving global image quality.

Key Points

- *Computed DWI improves global quality of prostate MRI.*
- *Computed DWI improves analysis of DWI images with decrease acquisition time.*
- *Computed DWI provides greater background suppression of parenchyma and improves conspicuity of suspicious lesion.*

Keywords Prostatic neoplasms · Diagnostic imaging · Magnetic resonance imaging · Diffusion-weighted MRI

Electronic supplementary material The online version of this article (https://doi.org/10.1007/s00330-019-06085-z) contains supplementary material, which is available to authorized users.

✉ Raphaele Renard-Penna
raphaele.renardpenna@aphp.fr

[1] Department of Radiology, Tenon Academic Hospital, AP-HP, Sorbonne Universités, Paris, France

[2] Department of Radiology, Pitié-Salpétrière Academic Hospital, AP-HP- Charles Foix, Sorbonne Universités, Paris, France

[3] CNRS, INSERM, LIB, Paris, France

[4] Department of Pathology, Hopital Tenon Academic Hospital, AP-HP, Sorbonne Universités, Paris, France

[5] Groupe de recherche clinique-UPMC n°5, Oncotype-Uro, Institut Universitaire de Cancérologie de l'UPMC, Pierre and Marie Curie Medical School, Sorbonne Universités, Paris, France

[6] Department of Biostatistics public health and medical information, Pitié-Salpétrière Academic Hospital, AP-HP, Sorbonne Universités, AP-HP, CIC-P 1421, Paris, France

Abbreviations

a-b2000	Acquired b 2000 images
a-DWI	Acquired diffusion-weighted images
ADC	Apparent diffusion coefficient
AUC	Area under the receiver operating curves
c-b2000	Computed b 2000 images
c-b2500	Computed b 2500 images
c-DWI	Computed diffusion-weighted images
DCE	Dynamic contrast-enhanced
DRE	Digital rectal examination
DWI	Diffusion-weighted imaging
IQR	Interquartile range
mp-MRI	Multiparametric magnetic-resonance imaging
NA	Non-applicable
PB	Prostate biopsy
PCa	Prostate cancer
PSA	Prostate serum antigen
PZ	Peripheral zone
ROI	Region of interest
SB	Standard biopsy
SNR	Signal-to-noise ratio (SNR)
T2W	T2-weighted
TB	Targeted biopsy
TRUS	Transrectal ultrasonographic
TZ	Transitional zone
US	Ultrasound

Introduction

Diffusion-weighted imaging (DWI) is a major component of MRI of the prostate, improving detection and characterization of prostate cancer (PCa) [1]. DWI is the essential sequence for assessment of the peripheral zone (PZ) in the PIRADS V2 score [2]. Because the highest proportion of prostate carcinoma arises within the PZ, satisfactory quality of DWI is mandatory. There is an on-going debate determining which *b*-values are appropriate for prostate DWI. Numerous studies reported the advantage of a *b*-value of 2000 s/mm^2 compared to a *b*-value of 1000 s/mm^2 [3–5], even though the ability at b 2000 to discriminate malignant from benign tissue in the PZ is limited due to a significant overlap of apparent diffusion coefficient (ADC) values [6]. However, depending upon the gradient performance, coil design, and software platform, DWI with *b*-values greater than 1000 s/mm^2 may otherwise be prohibitive in clinical practice because of longer acquisition time. Moreover, high *b*-value DWI suffers from poor quality due to poor signal-to-noise ratio (SNR) and geometric distortion. Computed DWI (c-DWI) is a calculation of a high *b*-value image from DWI images acquired with at least two different lower *b*-values [7]. In this way, disadvantages associated with direct high *b*-value measurements such as poor SNR and image distortion may be avoided. Computed DWI images require no additional acquisition time, and are generated automatically by the MR software at the time of image acquisition. It has been recently reported that high *b*-value c-DWI of the prostate could increase lesion conspicuity and image quality [3, 8–11]. With the widespread use of high filed 3 T without endorectal coil, rectal preparation and prostate volume may impact quality of diffusion imaging, and few studies had evaluated their impact on the quality of each diffusion approach [12].

Moreover, it is still unclear, whether high *b*-value c-DWI is clinically equivalent to high *b*-value a-DWI for detection of prostate cancer.

Our hypothesis is that c-DWI would make it possible to avoid the acquisition of a high-value of b and without any loss of information on tumor detection.

The aim of this study was to compare a-DWI (2000 s/mm^2) with different computed c-DWI (c-b2000, c-b2500) generated from a-DWI obtained with b-100, 400, and 800 s/mm^2 using a mono-exponential diffusion decay. Qualitative and quantitative image quality was evaluated as well as tumor detection and conspicuity in a multi-reader analysis using a 3 T MRI system without endo-rectal coil.

Material and methods

Study population

Our institutional radiology database was retrospectively queried to identify consecutive patients who underwent prostate MRI at our institution over a period of 8 weeks from January 1, 2017, to March 1, 2017. All the included patients had to fulfill the inclusion criterion for clinical indication of MRI of the prostate for suspicion of PCa (elevated PSA, DRE +, genetic susceptibility). Exclusion criteria included severe artifacts on DWI due to hip prosthesis, missing sequences in the protocol, or previous treatment for prostate cancer. Initially, 166 consecutive patients were included. Of these 166 patients, 42 patients were excluded (severe artifacts on DWI due to hip prosthesis $n = 5$, missing sequences in the protocol, $n = 28$, or previous treatment for prostate cancer, $n = 9$). The final study was based on 124 patients. Among those patients, 62 patients underwent prostate biopsy (PB). Mean age of the patients was 65.9 ± 9.4 years with a PSA level of 6.6 [5–8.95] ng/mL. This retrospective study was IRB approved. Written informed consent was waived. All MRI exams were prospectively analyzed by one radiologist with 15 years of experience in PCa using the PI-RADS V2 score.

Patients with PI-RADS score ≥ 3, suspicious DRE, genetic susceptibility underwent prostate biopsy.

When no lesion was described on MRI, 12 cores were obtained. When a focal lesion, defined with a PI-RADS score ≥ 3, was described, two additional targeted biopsies

were obtained using an MRI TRUS fusion system (Koelis). One senior pathologist with 10 years of experience in prostate pathology analyzed all the biopsies samples according to the 2014 International Society of Urological Pathology (ISUP) [13], and his rating was considered as the gold standard for sensitivity and specificity analysis.

MR technique

All MRI exams were performed using a 3 T clinical system (SIGNA™ Architect, GE Healthcare) using a 32-channel phased-array torso coil. Patients were advised to perform bowel preparation before the exam and to empty their bladder; 1 mg glucagon was administered intra muscularly to reduce peristaltic motion.

MRI protocol included 3DT2w images, high resolution Fov Optimized and Constrained Undistorted Single-Shot (FOCUSTM) DWI images with *b*-values of 100, 400, 800 (234 s), and 2000 s/mm^2 (additional 260 s). C-DWI images (2000 and 2500 s/mm^2) were then computed using GE software, derived from the three lower acquired *b*-value DWI images using a mono-exponential diffusion decay (additional table). Dynamic contrast-enhanced imaging of the prostate images after injection of 0.2 mL/kg of gadoterate meglumine (Dotarem, Guerbet), and delayed post-contrast fat-suppressed T1-weighted imaging of the pelvic were also performed for all examinations, although these were not evaluated for the purpose of this study.

Image analysis

A training meeting with the readers was organized before the start of the study, in order to reach agreement on each item's definition and values to be assigned. During this meeting, 10 prostate MRI exams, which are not included in the current study, were reviewed.

Then four radiologists E1, E2, J1, and J2 with respectively 3-, 2-, 1-, and 1-year experience in prostate MRI, blinded to clinical and pathologic information independently evaluated for each patient: the ADC map, the acquired b2000 images (a-2000), and the two computed DWI image sets (c-2000, c-2500) with a sequential reading. Each DW image sets were reviewed simultaneously with the axial T2-weighted images to guide anatomical location of findings on DW images. Abnormalities identified only on T2-weighted imaging were not recorded.

Image quality

For each DW images, the readers independently rated subjective image quality using a 5-point Likert scale for the following items: background signal suppression (5 = maximal signal suppression), anatomic clarity defined by zonal anatomical delineation (5 = excellent clarity), visualization of the prostatic capsule (5 = excellent visualization), and visualization of the peripheral-transition zone (TZ) boundary (5 = excellent visualization), absence of distortion (5 = no distortion), ghosting (5 = no ghosting), and overall image quality (5 = maximal quality). Quality of rectal preparation was also evaluated (5 = no distension).

Tumor detection

A suspicious lesion was defined as a focal increase in signal intensity within the PZ on DWI images or decreased voxel values on the ADC map, or a lenticular, homogeneous, moderately hypo-intense focal lesion on T2W in the TZ. When multiple lesions were identified, the reader was instructed to select only one lesion, defined as the index lesion, based on lesion's size, focality, and degree of signal alteration. For each detected lesion, lesion conspicuity on DWI and ADC map was assessed using a 5-point Likert scale based on signal intensity compared with the surrounding normal prostate tissue (5 = excellent conspicuity).

Quantitative measurements

SNR measurements

After the qualitative analysis, one of the four radiologists drew an ROI within an identified focal area of increased signal. A similar-sized ROI was also placed in an area of normal-appearing PZ without increased signal. The mean image intensity values of all ROIs were recorded. Tumor-to-PZ contrast was then calculated as (SItumor − SIPZ)/(SItumor + SIPZ), giving a value between 0 and 1 and that is greater in the setting of higher relative contrast [14, 15].

Geometric distortion

In order to study the impact of the prostate volume on image quality and artifacts according to each sequence and lesions detection, prostate volume was measured on T2W images by assuming an elliptical shape.

Diameters of the prostate on DWIs and on T2W images from left to right and from anterior to posterior at the level of the Veru Montanum were measured by one of the senior reader. A significant geometric distortion was defined if differences between DWIs and the TSE-T2W diameters were superior to 0.5 mm

Statistical analysis

All statistical analyses were undertaken using R 3.4.3 software (https://cran.r-project.org/). Statistical tests were two-sided and used a significance level of 0.05. Results are reported as

mean ± sd or median [Q1–Q3]. Characteristics of patients were described globally. Inter-observer agreement was evaluated computing intraclass correlation coefficient (ICC). The effect of sequence (acquired b2000, c-b2000, and c-b2500), adjusted on prostate volume and quality of rectal preparation, was assessed using linear mixed models to take into account the correlated nature of the data.

For quantitative image parameters study, a random intercept on the patient was introduced in the model. Both random intercept on the patient and on the reader were used for subjective image quality and conspicuity assessment. Pairwise comparisons of the sequences were subsequently computed through Tukey's HSD multiple comparison tests.

On the subgroup of patients undergoing a biopsy, detection of tumors was described by sequence, for each of the four radiologists. Sensitivity and specificity were calculated, with its 95% confidence interval computed by bootstrap using 10,000 iterations. Sensitivity was also computed on the subgroup of patients with clinically significant lesion (defined as Gleason score > 6).

Results

Subjective image quality (Table 1)

Considering all readers, c-b2000 and b2500 images had significant higher overall quality ($p < 0.001$), better background signal suppression ($p < 0.001$), better anatomic clarity ($p < 0.001$), and less distortion ($p < 0.001$), compared with a-b2000 DWI images. These conclusions remain unchanged when focusing only on more experienced readers. Increased ghosting was seen with c-b2000 and b2500 when considering all readers, whereas no difference of ghosting was found for experienced readers ($\beta(\text{sd}) = 0.01(0.02)$ for both computed DWIs, $p = 0.9$). Compared with c-b2000, c-b2500 had significantly better background signal suppression but increased ghosting (TukeyHSD $p < 0.001$ and $p = 0.002$ respectively), and non-significant differences for others subjective image quality items (TukeyHSD $p = 0.17$ for anatomic clarity, $p = 0.96$ for distortion, $p = 0.15$ for overall image quality). A prostate volume ≥ 50 cm^3 and a rectal quality score ≥ 4 were shown to increase significantly the overall quality assessment ($p = 0.018$ and $p < 0.001$ respectively) and improve distortion artifact assessment ($p = 0.007$ and $p < 0.001$ respectively).

Tumor detection (Table 2)

Among the 124 patients, 63 (50.8%) patients underwent MRI TRUS fusion biopsy after the MRI exam.

Forty-four patients (69.8%) had confirmed PCa at histopathology. The Gleason score distribution of the index lesions of the 44 patients was as follow 3 + 3 ($n = 19$), 3 + 4 ($n = 12$), 4 + 3 ($n = 4$), 4 + 4 ($n = 5$), 4 + 5 ($n = 2$), 5 + 4 ($n = 1$), 5 + 5 (1). Twenty-five patients had a clinically significant lesion, all detected prospectively (RRP) and were classified with PI-RADS > 3 (7 PIRADS 4, and 18 PIRADS 5). Similar values of sensitivity and specificity across readers were found regardless of the sequence. When focusing on Gleason 3 + 4 or greater, sensitivity across readers was also similar.

Tumor conspicuity (Tables 3 and 4)

Conspicuity was evaluated on the subgroup of patients who underwent a biopsy, when the reader had visualized a lesion. Compared with a-b2000 images, there was significantly greater conspicuity of the index lesions for both c-b2000 and c-b2500 images ($p < 0.001$). No

Table 1 Summary tables of the fixed effects estimates (standard errors) (β (se)) of the linear mixed models for all outcomes: subjective image quality items on the 124 MRI examinations with four readers

Subjective image quality item ($N = 124$ patients)	Overall quality		Anatomic clarity		Background signal suppression		Absence of distortion		Absence of ghosting	
	β (se)	p value	β (se)	p value	β (se)	p value	β (se)	p value	β (se)	p value
Intercept	3.38 (0.21)		2.71 (0.3)		3.53 (0.1)		4.11 (0.15)		4.91 (0.14)	
Effects of computed sequence (vs acquired b-2000)										
c b-2000	0.43 (0.04)	< 0.001	0.45 (0.05)	< 0.001	0.33 (0.04)	< 0.001**	0.28 (0.04)	< 0.001	− 0.33 (0.03)	< 0.001**
c b-2500	0.49 (0.04)		0.51 (0.05)		0.73 (0.04)		0.28 (0.04)		− 0.43 (0.03)	
Other fixed effects										
Prostate volume ≥ 50	0.15 (0.06)	0.018	0.23 (0.09)	0.009	0.17 (0.08)	0.041	0.15 (0.05)	0.007	0.05 (0.03)	0.169
Rectal quality score ≥ 4	0.22 (0.04)	< 0.001	0.12 (0.05)	0.018	0.1 (0.05)	0.048	0.22 (0.04)	< 0.001	0.05 (0.03)	0.133

**For these outcomes, Tukey's HSD multiple comparison test shown significant p at least < 0.05 for comparison between c b-2000 and c b-2500

For other outcomes, it is not significantly different

Table 2 Diagnostic Sensitivity and specificity for all Tumor, and clinically significant tumor

Diagnostic performance % (IC95%) $N = 62$ patients	Reader	b2000	b2000 C	b2500 C
Sensitivity (all PB)	E1	82 (36/44) [69–93]	82 (36/44) [70–93]	82 (36/44) [70–93]
	E2	73 (32/44) [59–85]	75 (33/44) [62–87]	77 (34/44) [64–89]
	J1	77 (33/43) [64–89]	77 (34/44) [64–89]	77 (34/44) [64–89]
	J2	77 (34/44) [64–89]	77 (34/44) [64–89]	77 (34/44) [64–89]
Sensitivity (Gleason > 6)	E1	96 (24/25) [88–100]	96 (24/25) [88–100]	96 (24/25) [88–100]
	E2	88 (22/25) [76–100]	92 (23/25) [80–100]	96 (24/25) [88–100]
	J1	92 (23/25) [80–100]	88 (22/25) [76–100]	88 (22/25) [76–100]
	J2	96 (24/25) [88–100]	96 (24/25) [88–100]	96 (24/25) [88–100]
Specificity (all PB)	E1	58 (11/19) [35–80]	58 (11/19) [35–80]	58 (11/19) [33–80]
	E2	63 (12/19) [40–85]	63 (12/19) [40–85]	47 (10/19) [24–71]
	J1	68 (13/19) [46–89]	68(13/19) [47–89]	68 (13/19) [47–89]
	J2	74 (14/19) [52–93]	74 (14/19) [53–92]	74 (14/19) [52–94]

significant difference in conspicuity was evidenced between c-b2000 and c-b2500. No improvement of tumor conspicuity with prostate volume ≥ 50 cm^3 and a rectal quality score ≥ 4 $p = 0.20$) on the subgroup of patients with biopsy with representative case is shown in (Fig. 1).

Quantitative analysis of contrast ratio and distortion (Table 5)

Non-acquisition of high *b*-value a-DWI reduced total acquisition time by 260 s per patient.

Quantitative tumor to PZ contrast was significantly greater on c-b2000 and c-b2500 images than on a-b2000 ($p < 0.001$). Figure 2 shows the boxplots of contrast ratio measurements.

Left to right distortion was higher on a-b2000 than on c-b2000 and c-b2500 ($p = 0.02$) but there was no statistically significant differences on anterior to posterior distortion between all different DWI sequences ($p = 0.79$).

Discussion

We have demonstrated that c-DWI may provide high quality images when analyzed by readers with varying experiences,

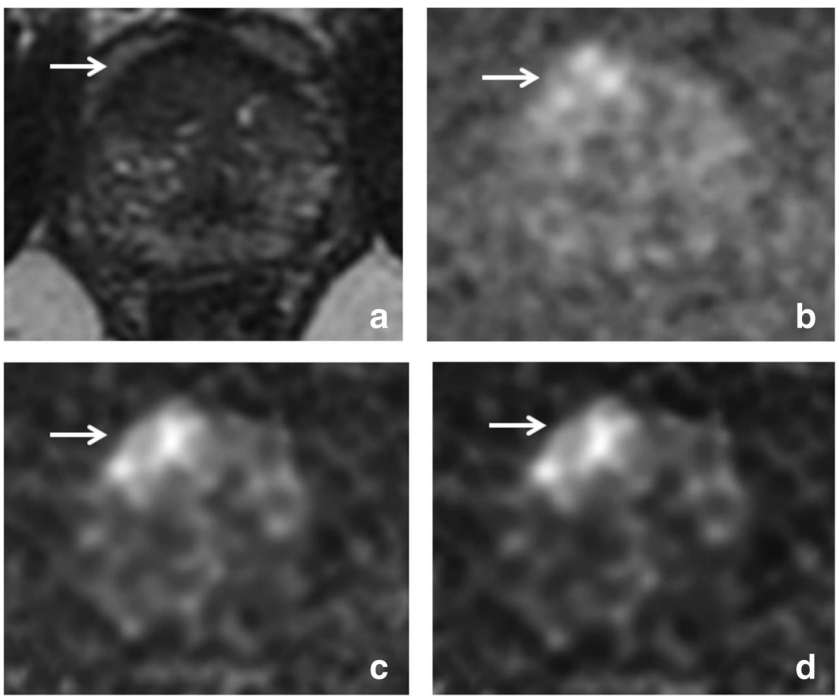

Fig. 1 Axial T2-weighted MRI image (**a**) shows a large hypointense signal lesion developed in the transitional zone, PIRADS 5. This lesion is more clearly identified in axial calculated b 2000 and b 2500 weighted images (**c** and **d**) than in acquired b 2000 (**b**) diffusion-weighted image. Calculated b2500 diffusion-weighted image (D) has the best conspicuity for lesion detection

Table 3 Lesion conspicuity scores with acquired b2000, computed b2000, and computed b2500

Variable	b2000 (A)	b2000 C (B)	b2500 C (C)	*p* global	*p* A vs B	*p* A vs C	*p* B vs C
Conspicuity	3.93 (0.28)	4.22 (0.28)	4.31 (0.28)	< 0.001	< 0.001	< 0.001	0.176
Conspicuity (Gleason ≥ 3 + 4)	4.38 (0.28)	4.52 (0.28)	4.6 (0.28)	0.029	0.21	0.024	0.30

with a significant decrease time acquisition of 220 s per patient. For all subjective quality assessments, except ghosting, the readers found that c-DWI improved significantly the overall image quality compared to a-b2000. Computed b 2500 was significantly superior to c-b2000 for background signal suppression.

Regarding the diagnostic performance for PCa detection, we have shown that c-DWI has comparable tumor detection rate as a-DWI. The detection rate for significant cancer was excellent (E1 96%, E2 92 to 96%, J1 88%, J2 96%) with a shortened protocol consisting of T2 and b 2000. We also demonstrated that, when compared with a-b2000 images, there was significant greater conspicuity of the index lesion for both c-b2000 and c-b2500 and that the tumor to PZ contrast ratio was significantly higher. No difference in conspicuity between c-b2000 and c-b2500 was found.

Our results are in accordance with previous published studies, however the number of patients and reader is superior, and the calculation of our computed DWI is obtained with 3 low *b*-values < 1000 s/mm^2. Bittencourt et al, compared acquired and c-b1400 and showed that overall image quality was rated significantly better and signal intensity ratios were significantly higher [11]. Rosenkrantz et al compared image quality and tumor detection of acquired and c-b1500 DWI in 49 patients with two readers and found a greater background signal suppression, less distortion, and fewer artifacts using computed versus acquired [9]. A higher conspicuity and tumor to PZ contrast ratio for computed high *b*-values was an expected finding, as images are less affected by poor SNR and geometric distortion [16]. Computed DWI is more likely than acquired images to highlight differences in signal intensity between cancerous and non-cancerous tissue on images with high *b*-values. Feuerlein et al compared CNRs of very high computed *b*-values > 2000 s/mm^2 and the respective ADC map in 14 patients and concluded that c-DWI was able to provide better contrast between prostate tumor and background tissue than is a standard ADC map on a 3 T with endo-rectal coil. However authors evaluated the diagnostic capability and the contrast ratios of cancerous and non-cancerous lesions without qualitative criteria analysis [17]. Ueno et al evaluated the clinical diagnostic ability of c-DWI for prostate cancer in 80 patients, with two radiologists and found that c-DWIs with b-2000 were not superior or inferior to acquired DWIs. However in this study, c-DWI was calculated only with two *b*-values (b0 and b1000 s/mm^2) instead of 3 low *b*-values (< 1000 s/mm^2) [18].

The better image quality of c-DWI, the better conspicuity and the higher tumor to PZ contrast ratio did not translate into improved tumor detection. Both acquired and calculated high *b*-value imaging increased specificity of tumor detection while maintaining sensitivity for high grade tumor. Therefore high *b*-values have the potential to reduce the number of insignificant cancers detected by biopsy. Indeed, the ideal test for prostate cancer detection would be identifying a high proportion of men who would benefit from treatment and minimize the identification of men with clinically insignificant cancer in order to prevent overtreatment. In this study, among the patients who underwent MRI-targeted biopsy, detection rates for significant cancers were excellent with a shortened protocol consisting of T2 and b 2000 with slight difference with experience level of the readers.

Table 4 Summary tables of the fixed effects estimates (standard errors) (β (se)) of the linear mixed models for all outcomes: lesion's conspicuity

Subjective image quality item	Conspicuity (all PB) (N = 44 patients)		Conspicuity (Gleason > 6) (N = 24 patients)	
	β (sd)	*p* value	β (sd)	*p* value
Intercept	3.89 (0.29)		4.21 (0.29)	
Effects of computed sequence (vs acquired b-2000)				
c b-2000	0.29 (0.07)	< 0.001	0.13 (0.08)	0.030
c b-2500	0.38 (0.07)		0.22 (0.08)	
Other fixed effects				
Prostate volume ≥ 50	− 0.03 (0.19)	0.85	0.29 (0.19)	0.19
Rectal quality score ≥ 4	0.1 (0.08)	0.20	0.08 (0.1)	0.39

Table 5 Summary tables of the fixed effects estimates (standard errors) (β (se)) of the linear mixed models for all outcomes: objective image quality item

Objective image quality item	Distortion AP ($N = 124$ patients)		Distortion Larg ($N = 124$ patients)		Contrast ratio ($N = 44$ patients)	
	β (se)	p value	β (se)	p value	β (se)	p value
Intercept	4.69 (0.21)		4.19 (0.41)		0.21 (0.04)	
Effects of computed sequence (vs acquired b-2000)						
c b-2000	− 0.26 (0.03)	< 0.001 **	− 0.86 (0.33)	0.017	0.25 (0.03)	< 0.001 **
c b-2500	− 0.39 (0.03)		− 0.81 (0.33)		0.39 (0.03)	
Other fixed effects						
Prostate volume ≥ 50	0.04 (0.04)	0.251	− 0.27 (0.39)	0.50	0.07 (0.04)	0.063
Rectal quality score ≥ 4	0.08 (0.03)	0.007	− 0.98 (0.4)	0.015	0.02 (0.04)	0.51

**For these outcomes, Tukey's HSD multiple comparison test shown significant p at least < 0.05 for comparison between c b-2000 and c b-2500

For other outcomes, it is not significantly different

Because we did not use endorectal coil, we wanted to evaluate whether rectal distension impacted on image quality of acquired or computed diffusion images. We found that absence of rectal distension, as well as a prostate volume > 50 cm^3 were significantly associated with a higher quality of DWI images, whether it was acquired or computed DWIs. There are limited number of previous studies looking at the issue of rectal preparation and prostate volume and quality of DWI. Caglic et al found that rectal distension had a negative effect on the quality of diffusion imaging [19]. Padhani et al showed that rectal movements are related to rectal distension and may result in significant displacement of the prostate gland and consequently alter the image quality [20].

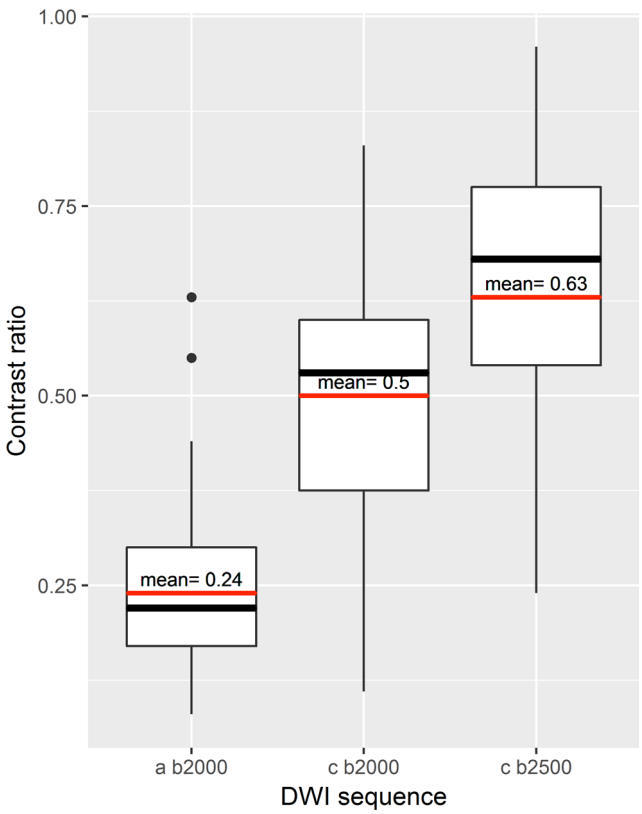

Fig. 2 Contrast ratio: boxplots of contrast ratio measurements

There are several limitations of this study. First, the gold standard was MR/TRUS fusion-guided biopsy instead of radical prostatectomy specimens. Whereas pathologic findings from prostatectomy would have been more accurate, the approach used is reasonable; MR/TRUS fusion-guided biopsies are becoming a gold standard with a very high accuracy [1]. In our study, tumor detection could not be assessed in the whole sample of 124 patients, but only on a subgroup of 63 patients undergoing biopsies. Second, we only assessed two computed DWI, b-2000 and b 2500 images. We selected those b-values because we wished to compare c-DWI with a-DWI obtained at an identical b-value and we were able to obtain direct DWI at a b-value of 2000 s/mm^2. Moreover, Vural et al compared different c-DWIs (b 1500, b 2000 and b 3000 s/mm^2) and found that c-b2000 was the preferable image set in localizing cancer in prostate gland [21]. Third, all sequences for a given patient were analyzed consecutively. We made this pragmatic choice due to logistical constraints and all readers were told to analyze each sequence independently from others.

To conclude, we have demonstrated that the c-DWI images at b-values greater than 2000 s/mm^2 may provide images with highest ratings of quality, except for ghosting, while maintaining comparable prostate cancer detection rate, with shorter time acquisition and so decreasing examination costs for readers of varying experiences. Our study suggested that c-DWI might be routinely incorporated into prostate MRI protocols and replace a standard a-DWI at high b-value.

Funding The authors state that this work has not received any funding.

Compliance with ethical standards

Guarantor The scientific guarantor of this publication is Dr Raphaele Renard-Penna.

Conflict of interest The authors of this manuscript declare no relationships with any companies, whose products or services may be related to the subject matter of the article.

Statistics and biometry One of the authors has significant statistical expertise.

Informed consent Written informed consent was obtained from all subjects (patients) in this study.

Ethical approval Institutional Review Board approval was obtained.

Methodology
- retrospective
- performed at one institution

References

1. Kasivisvanathan V, Rannikko AS, Borghi M et al (2018) MRI-targeted or standard biopsy for prostate-cancer diagnosis. N Engl J Med 378:1767–1777
2. Weinreb JC, Barentsz JO, Choyke PL et al (2016) PI-RADS prostate imaging - reporting and data system: 2015, version 2. Eur Urol 69:16–40
3. Rosenkrantz AB, Hindman N, Lim RP et al (2013) Diffusion-weighted imaging of the prostate: comparison of b1000 and b2000 image sets for index lesion detection. J Magn Reson Imaging 38:694–700
4. Ohgiya Y, Suyama J, Seino N et al (2012) Diagnostic accuracy of ultra-high-b-value 3.0-T diffusion-weighted MR imaging for detection of prostate cancer. Clin Imaging 36:526–531
5. Ueno Y, Kitajima K, Sugimura K et al (2013) Ultra-high b-value diffusion-weighted MRI for the detection of prostate cancer with 3-T MRI. J Magn Reson Imaging 38:154–160
6. Kitajima K, Kaji Y, Kuroda K, Sugimura K (2008) High b-value diffusion-weighted imaging in normal and malignant peripheral zone tissue of the prostate: effect of signal-to-noise ratio. Magn Reson Med Sci 7:93–99
7. Maas MC, Futterer JJ, Scheenen TW (2013) Quantitative evaluation of computed high B value diffusion-weighted magnetic resonance imaging of the prostate. Invest Radiol 48:779–786
8. Glaister J, Cameron A, Wong A, Haider MA (2012) Quantitative investigative analysis of tumour separability in the prostate gland using ultra-high b-value computed diffusion imaging. Conf Proc IEEE Eng Med Biol Soc 2012:420–423
9. Rosenkrantz AB, Chandarana H, Hindman N et al (2013) Computed diffusion-weighted imaging of the prostate at 3 T: impact on image quality and tumour detection. Eur Radiol 23:3170–3177
10. Ueno Y, Takahashi S, Ohno Y et al (2015) Computed diffusion-weighted MRI for prostate cancer detection: the influence of the combinations of b-values. Br J Radiol 88:20140738
11. Bittencourt LK, Attenberger UI, Lima D et al (2014) Feasibility study of computed vs measured high b-value (1400 s/mm^2) diffusion-weighted MR images of the prostate. World J Radiol 6:374–380
12. Caglic I, Hansen NL, Slough RA, Patterson AJ, Barrett T (2017) Evaluating the effect of rectal distension on prostate multiparametric MRI image quality. Eur J Radiol 90:174–180
13. Epstein JI, Egevad L, Amin MB et al (2016) The 2014 International Society of Urological Pathology (ISUP) consensus conference on Gleason grading of prostatic carcinoma: definition of grading patterns and proposal for a new grading system. Am J Surg Pathol 40:244–252
14. Cornfeld DM, Israel G, McCarthy SM, Weinreb JC (2008) Pelvic imaging using a T1W fat-suppressed three-dimensional dual echo Dixon technique at 3T. J Magn Reson Imaging 28:121–127
15. Hori M, Kim T, Onishi H et al (2011) Uterine tumors: comparison of 3D versus 2D T2-weighted turbo spin-echo MR imaging at 3.0 T–initial experience. Radiology 258:154–163
16. Blackledge MD, Leach MO, Collins DJ, Koh DM (2011) Computed diffusion-weighted MR imaging may improve tumor detection. Radiology 261:573–581
17. Feuerlein S, Davenport MS, Krishnaraj A, Merkle EM, Gupta RT (2015) Computed high b-value diffusion-weighted imaging improves lesion contrast and conspicuity in prostate cancer. Prostate Cancer Prostatic Dis 18:155–160
18. Ueno Y, Takahashi S, Kitajima K et al (2013) Computed diffusion-weighted imaging using 3-T magnetic resonance imaging for prostate cancer diagnosis. Eur Radiol 23:3509–3516
19. Czarniecki M, Caglic I, Grist JT et al (2018) Role of PROPELLER-DWI of the prostate in reducing distortion and artefact from total hip replacement metalwork. Eur J Radiol 102:213–219
20. Padhani AR, Khoo VS, Suckling J, Husband JE, Leach MO, Dearnaley DP (1999) Evaluating the effect of rectal distension and rectal movement on prostate gland position using cine MRI. Int J Radiat Oncol Biol Phys 44:525–533
21. Vural M, Ertas G, Onay A et al (2014) Conspicuity of peripheral zone prostate cancer on computed diffusion-weighted imaging: comparison of cDWI1500, cDWI2000, and cDWI3000. Biomed Res Int 2014:768291